Inorganica Chimica Acta, *88* (1984) 75–81

Structural and Spectroscopic Studies of the $[Mo_2(\mu_4\text{-}S_2)(\mu_2\text{-}SO_2)(CN)_8]^{4-}$ anion, a Complex with a Mo–Mo Bond and a Distorted Confacial Bis-Bipyramidal Framework†

JEAN-MARIE MANOLI, JEAN-MARIE BRÉGEAULT, CLAUDE POTVIN

Laboratoire de Cinétique Chimique, Université P. et M. Curie, 1, rue Guy de la Brosse, 75005 Paris, France

and GENEVIÈVE CHOTTARD

Département de Recherches Physiques, Université P. et M. Curie, 4, place Jussieu, 75230 Paris, France

Received January 4, 1984

The aerial oxidation of $K_6[Mo_2(\mu_2\text{-}S)_2(CN)_8]\cdot 4H_2O$ dissolved in water gives $K_4[Mo_2(\mu_4\text{-}S_2)(\mu_2\text{-}SO_2)(CN)_8]\cdot 2.5H_2O$ (1) together with by-products. The structure of the deep purple crystals of (1) contains two crystallographically-independent anions which possess a distorted confacial bis-bipyramidal framework with a Mo–Mo interaction. The space group is $P\bar{1}$ triclinic with cell dimensions $a = 10.525(3)$, $b = 16.189(5)$, $c = 15.823(5)$ Å, $\alpha = 106.69(3)$, $\beta = 101.53(3)$, $\gamma = 95.18(3)°$, $D_x = 2.05$ g cm^{-3} for $Z = 4$. The structure was solved by direct method to $R = 0.053$ for 7765 reflections ($F_o^2 > 3\sigma(F_o^2)$). The Mo–Mo distances are 2.691(1) and 2.794(1) Å. The anion has been investigated spectroscopically (UV/visible, IR and resonance Raman). The absorption band in the visible region (550 nm; $\epsilon \simeq 4000$ mol^{-1} l^{+1} cm^{-1}) is assigned to the charge transfer transition $S \rightarrow d$ (Mo) or to the Mo–Mo σ–σ^* transition. An assignment of the low frequency Raman bands is proposed, based on their excitation profiles.

Introduction

As part of our study on oxidation processes we became interested in investigating the metal complex–dioxygen interaction. Of the many reported metal complex oxidations by O_2 (see, for example [1–9]) or other oxidizing agents, the oxidation of sulfido-complexes appeared as one of the most attractive for the formation of new chemical species. Vahrenkamp *et al.* were the first to report fixation of sulfur monoxide in a cluster, $Fe_3(CO)_9(S)(SO)$, the oxidizing agent being H_2O_2 [10]. We also recently reported [11] that aerial oxidation of the $[Mo_2(\mu\text{-}S)_2(CN)_8]^{4-}$ ion leads to the formation of a purple diamagnetic complex $[Mo_2(\mu_4\text{-}S_2)(\mu_2\text{-}SO_2)(CN)_8]^{4-}$. If the metal–metal bond is not considered, this 'Mo_2 anion' contains two molybdenum centers with a distorted pentagonal bipyramidal coordination geometry. The Mo–Mo separation of 2.730(4) Å may imply the existence of a single metal–metal bond between these molybdenum(III) atoms. To our knowledge [12], this geometry is unique: it is the first type of bridging *via* one edge (S_2^{2-}) and one axial site (sulfur in SO_2), such that a confacial configuration is defined.

In spite of the growing interest in compounds with multiple metal to metal bonds [13–18], there are few examples concerning physicochemical studies of single metal–metal bonds. When the metal atoms are bridged by ligands, the conclusion that metal–metal bonds exist is less obvious, but generally follows from such evidence as the closeness of approach of the metal atoms, the lack of unpaired electrons, and the similarity to a compound in which there are no bridges.

The difficulties encountered in attempting to identify the oxidized species in aqueous medium led us to use tetraphenylphosphonium chloride for the isolation of the anionic species [11]. The recent X-ray diffraction studies of Bau and co-workers [19, 20] concerning the $[HW_2(CO)_{10}]^-$ and the $[Fe(CO)_4]^{2-}$ anions, which showed a dramatic influence of the nature of the counterion, led us to speculate as to whether this remarkable 'Mo_2 anion' might adopt different geometries in different crystalline salts (see $[Ni(CN)_5]^{3-}$ [21] with cyanide ion as ligand). Therefore, our efforts were directed towards the isolation of a pure potassium salt of the 'Mo_2 anionic' species. We report here the crystal structure of $K_4[Mo_2(\mu_4\text{-}S_2)(\mu_2\text{-}SO_2)(CN)_8]\cdot 2.5H_2O$ (*1*). The structural data are in agreement with previous work concerning $(PPh_4)_4[Mo_2(\mu_4\text{-}S_2)(\mu_2\text{-}SO_2)(CN)_8]\cdot 6H_2O$ (*2*) [11]. We can attempt therefore to

†Presented at the International Conference on the Chemistry of Chromium, Molybdenum and Tungsten University of Sussex, Brighton, U.K., 5–8 July 1983; sponsored by the Royal Society of Chemistry.

0020-1693/84/$3.00

characterize the metal–metal bond more thoroughly by means of a spectroscopic investigation.

Experimental

Preparation of Crystals of $K_4[Mo_2(\mu_4\text{-}S_2)(\mu_2\text{-}SO_2)(CN)_8]\cdot 2.5H_2O$ (1)

The complex was prepared by aerial oxidation of $K_6[Mo_2(\mu_2\text{-}S)_2(CN)_8]\cdot 4H_2O$ [22], (1 g) dissolved in water (10 cm^3). Potassium cyanide and other by-products were extracted with methanol after 4-days oxidation at room temperature to give a purple oil. A further addition of H_2O to the oil gave a purple solution, which was filtered and allowed to stand. Dark purple crystals of (*1*) were obtained by fractional crystallization (27 °C) (σ(SO): 955, 1010 and 1125 cm^{-1}).

Single-Crystal X-Ray Data Collection and Structure Determination

Triclinic symmetry was established by precession and Weissenberg photography. Space group $P\bar{1}$ was assumed and the subsequent successful elucidation and refinement of the structure vindicated this assumption. A well-formed crystal was selected for data collection, mounted on the end of a glass fiber, and transferred to a Philips PW 1100 four-circle diffractometer.

Cell constants and other pertinent data are presented in Table I. No intensity decay was observed in the step-scan mode with subsequent computer analysis of the recorder profiles by means of Coppens' program [23]. Because difficulties were encountered, more details than usual are provided to describe the solution and refinement of the structure.

The structure was solved by direct methods using the MULTAN 77 program [24]. Normalized structure factor amplitudes were generated in a standard manner from $|F_o(h\,k\,l)|$ values. The E map generated from the phase set with the best combined figure of merit showed the positions of the molybdenum atoms and part of the sulfur atoms between them. Subsequent Fourier syntheses [25] revealed the locations of the two discrete anions of formula $[Mo_2(CN)_8(\mu_4\text{-}S_2)(\mu_2\text{-}SO_2)]^{4-}$ together with six K^+, four water molecules and also some other unidentified peaks. This model was refined by least-squares analysis [26], using anisotropic thermal parameters for all atoms, and led to an R value of 0.107 for 7765 reflections. The stoichiometry of 6 K^+ in the asymmetric unit was somewhat surprising in view of the chemical analysis. This suggested the presence of disorder; the unknown peaks could be potassium sites with partial occupancy factors. A model with five partially occupied sites (KD1 to KD5) for 2 K^+ was proposed, the occupancy factors being fixed at values corresponding to the relative peak heights of fully and partially occupied sites of potassium in the Fourier maps. Refinement of this model led to reasonable distances and temperature factors. A subsequent Fourier difference map showed residual electron densities and was interpreted as a nearly half-populated site for a fifth water molecule (OH51, OH52).

The final model for the structure, described by 567 variable parameters, was refined by using the 7765 data in three blocks (for computing economy): one containing the first anion, the second containing the second anion and the last with the ordered and disordered K^+ cations and the water molecules. The final values for R and R_w are 0.053 and 0.076. Values of the atomic scattering factors for all atoms were obtained from the usual source [27].

The anisotropic thermal parameters for all atoms, provided as U_{ij}, and the observed and calculated structure factors are available as supplementary material. The final positional parameters are listed in Table II.

Raman Spectra. Absorption Spectrum

The Raman data were obtained on H_2O/CH_3OH(3:1) solutions at 10^{-3} mol l^{-1}, using a rotating cell. The Raman spectrometer was a Coderg DH 800 double monochromator equipped with a RCA C 31034 phototube. Ar^+ and Kr^+ CW laser excitation and rhodamine 6 G dye laser excitation were used.

TABLE I. Experimental Details of the X-Ray Diffraction Study of $K_4[Mo_2(\mu_4\text{-}S_2)(\mu_2\text{-}SO_2)(CN)_8]\cdot 2.5H_2O$.

(A) Crystal parameters at 23 °C

Crystal class: triclinic	Space group: $P\bar{1}$
a, b, c, Å: 10.525(3), 16.189(5), 15.823(5)	
α, β, γ, deg.: 106.69(3), 101.53(3), 95.18(3)	
V, Å^3: 2498.8	mol. wt.: 729.66
Z: 4	
ρ(calcd): 1.94 g cm^{-3}	ρ(obsd)[a]: 2.00 g cm^{-3}

(B) Experimental conditions for data processing

Diffractometer: Philips PW 1100
Radiation: Mo Kα (λ = 0.71069 Å) graphite monochromated
abs: μ = 20.6 cm^{-1}
Scan width, deg.: 1.30
Scan speed, deg./s: 0.025
Stds: three reflections $(25\bar{9})$, (444) and $(\bar{2}5\bar{9})$ measured every hour
2θ limits, deg.: $6 \leqslant 2\theta \leqslant 56°$
No. of reflections collected: 12566, yielding 7765 symmetry independent data with $F_o^2 > 3\sigma(F_o^2)$
Corrn.: Lorentz, polarisation, anomalous dispersion for Mo[b], no absorption correction was applied
Final no. of parameters varied: 567
R: 0.053 R_w: 0.076

[a]By flotation in benzene–carbon tetrachloride mixture. [b]Reference [27].

TABLE II. Final Positional Parameters in $K_4[Mo_2(\mu_4\text{-}S_2)(\mu_2\text{-}SO_2)(CN)_8]\cdot 2.5H_2O$.

Atom	x	y	z
Mo1	0.72599(7)	0.79719(5)	0.77731(5)
Mo2	0.46604(7)	0.78330(5)	0.71093(5)
Mo3	0.37931(7)	0.20249(5)	0.66495(5)
Mo4	0.64934(7)	0.20712(5)	0.72324(5)
S11	0.5626(2)	0.7122(1)	0.8135(1)
S12	0.6288(2)	0.8070(1)	0.6275(1)
S13	0.6234(2)	0.9111(1)	0.7312(1)
O11	0.5437(7)	0.7407(4)	0.9076(4)
O12	0.5558(7)	0.6156(4)	0.7823(4)
C11	0.9107(9)	0.8610(6)	0.7683(6)
N11	1.0088(9)	0.8965(7)	0.7701(7)
C12	0.7724(9)	0.6783(6)	0.6955(6)
N12	0.800(1)	0.6150(6)	0.6554(6)
C13	0.8488(9)	0.7436(6)	0.8723(6)
N13	0.9169(9)	0.7258(6)	0.9239(6)
C14	0.761(1)	0.8971(6)	0.9063(6)
N14	0.7867(9)	0.9500(6)	0.9753(6)
C21	0.4175(9)	0.8724(6)	0.8233(6)
N21	0.3946(9)	0.9204(6)	0.8874(6)
C22	0.3283(9)	0.8350(6)	0.6249(6)
N22	0.2515(9)	0.8626(6)	0.5850(6)
C23	0.292(1)	0.7191(7)	0.7265(7)
N23	0.192(1)	0.6853(8)	0.7314(9)
C24	0.4236(9)	0.6580(6)	0.6059(6)
N24	0.4042(9)	0.5904(6)	0.5554(6)
S31	0.5240(2)	0.3104(1)	0.7876(1)
S32	0.5243(2)	0.1470(2)	0.5657(1)
S33	0.4901(2)	0.0744(1)	0.6443(2)
O31	0.5136(7)	0.3208(5)	0.8825(4)
O32	0.5501(6)	0.4008(4)	0.7807(5)
C31	0.3085(9)	0.1467(6)	0.7581(6)
N31	0.2621(8)	0.1185(6)	0.8054(6)
C32	0.2357(9)	0.2800(6)	0.7118(6)
N32	0.1543(9)	0.3159(6)	0.7354(6)
C33	0.3677(9)	0.2956(6)	0.5903(8)
N33	0.3538(9)	0.3454(6)	0.5522(6)
C34	0.2109(9)	0.1260(6)	0.5614(6)
N34	0.1144(8)	0.0919(6)	0.5108(6)
C41	0.6513(9)	0.1510(6)	0.8309(7)
N41	0.6543(9)	0.1203(7)	0.8899(7)
C42	0.7283(9)	0.3000(6)	0.6656(6)
N42	0.7744(9)	0.3472(6)	0.6356(7)
C43	0.8110(9)	0.1375(6)	0.6975(6)
N43	0.9043(9)	0.1081(6)	0.6898(6)
C44	0.7952(9)	0.2934(6)	0.8354(7)
N44	0.872(1)	0.3422(6)	0.8940(7)
K1	0.4324(2)	0.1045(2)	−0.0442(1)
K2	−0.0789(2)	0.0133(1)	0.3500(1)
K3	0.4195(2)	−0.4752(1)	0.3668(2)
K4	0.0543(2)	−0.2167(2)	0.4285(2)
K5	−0.0789(2)	−0.2320(2)	0.1228(2)
K6	−0.1614(3)	0.1365(2)	0.0558(2)
KD1[a]	0.3023(5)	−0.4767(3)	0.0100(3)
KD2[a]	−0.0372(5)	0.4070(3)	0.1856(4)
KD3[a]	−0.1699(7)	−0.4566(5)	0.4672(5)
KD4[a]	−0.192(1)	0.5151(8)	0.407(1)
KD5[a]	−0.280(1)	0.3044(9)	0.0508(8)
O1	0.0332(9)	−0.0870(5)	0.0927(6)
O2	−0.3166(8)	−0.3352(6)	0.0337(5)
O3	0.2113(9)	0.4773(6)	0.1649(7)
O4	0.028(1)	0.283(1)	0.4451(8)
O51[a]	−0.088(1)	−0.456(1)	0.113(2)
O52[a]	−0.021(1)	−0.455(1)	0.183(2)

Estimated standard deviations of least significant figures are given in parentheses.

[a]Atoms in crystal disorder with partial occupancy factors: KD1 (0.5); KD2 (0.5); KD3 (0.5); KD4 (0.25); KD5 (0.25); O51 (0.6); O52 (0.4).

The Raman intensities were measured relative to the 1020 cm^{-1} band of methanol and have been corrected for the ν^4 law, re-absorption and instrument response.

The absorption spectrum at low temperature was measured on a polyvinyl alcohol film.

Results and Discussion

X-Ray Crystallographic Results

The unit cell of (*1*) contains one pair of crystallographically-independent anions. An ORTEP drawing of the two independent anions is shown in Fig. 1. Table III presents selected bond distances and angles for both anions; structurally they are very similar and possess only C_1 symmetry. It is of interest to compare the present compound (*1*) with the analogous dimeric molybdenum cyano complexes already published (*2*), in which the cation is different [11]. The two complexes are identical with respect to: (i) the bridging ligands (a disulfur S_2^{2-} and a SO_2 bound by the sulfur atom); (ii) the geometry of the coordination polyhedron about each metal atom. If the metal–metal bond is not considered, each molybdenum has a distorted pentagonal bipyramidal coordination geometry. The ORTEP view of the anions shows that they possess a distorted confacial bis-bipyramidal framework with weak metal–metal interaction. The cyanide groups C11 N11, C22 N22, C43 N43 and C34 N34 occupy the other axial positions so that the girdle axes are S11 Mo1 C11 N11, S11 Mo2 C22 N22, S31 Mo4 C43 N43 and S31 Mo3 C34 N34. The carbon atoms and the sulfur atoms (disulfido ligand) of the pentagonal girdle are nearly co-planar, none of them being displaced more than 0.12 Å from the least square planes (see Supplementary Material).

A number of complexes have been reported which contain an SO_2 group bridging two metals, and bound only through S [28]. The title complex contains a Mo–SO_2–Mo bridge supported by another bridging ligand (S_2^{2-}) and a possible metal–metal bond. To our knowledge, only one structure of this type exists: $\{[(Cp)Fe(CO)]_2(CO)(SO_2)\}$ [29]. In this

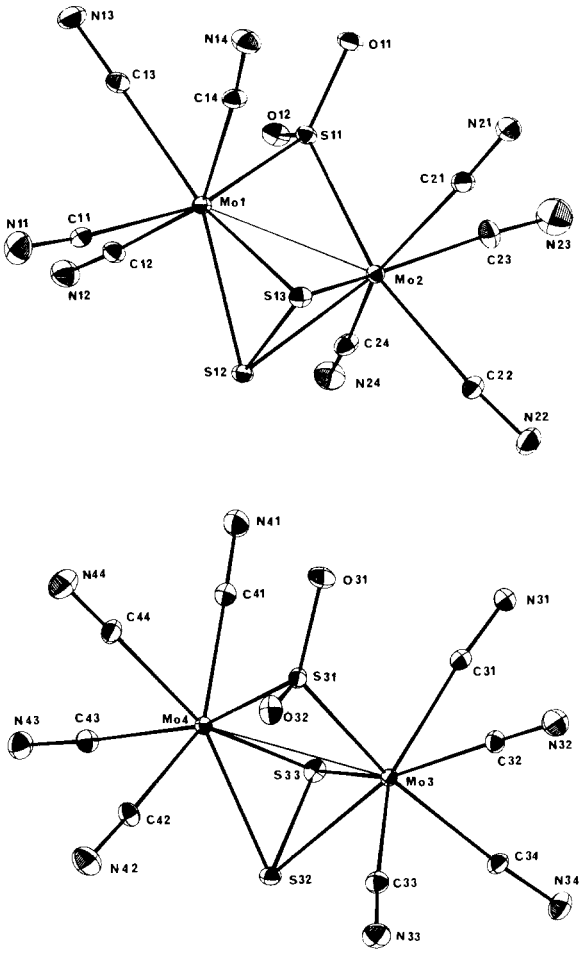

Fig. 1. Perspective representation of the two independent anions of $K_4[Mo_2(\mu_4\text{-}S_2)(\mu_2\text{-}SO_2)(CN)_8]\cdot 2.5H_2O$. The vibrational ellipsoids are drawn at the 50% probability level. The labeling scheme is also shown.

bonding mode, SO_2 can act as a four electron donor ligand, with two orbitals forming pair bonds with the metals. The symmetrical nature of the bridging ligands is reflected by the equivalent Mo–S bond lengths (Mo–SO_2 distances ranging from 2.351(2) to 2.370(2); Mo–S_2^{2-} distances ranging from 2.429-(2) to 2.449(2)). The S–S bond distances are characteristic of a normal single bond and are in general agreement with the S–S distances already observed in molybdenum compounds containing this bridging anion [30–31]. An interesting aspect of this structure is the dihedral angle of 89.6° between the plane containing the bridging ligands and a plane containing the two metals and the sulfur atom of SO_2, this angle reflecting the way in which the bridging ligands bissect the anion.

As far as the Mo–C bond lengths are concerned there is no significant variation in any of the distances or angles in the Mo–C≡N moiety over the sixteen cyanide groups found in these two independent anions. The mean values are listed in Table III. Clearly, there is a small but persistent deviation from linearity in the Mo–C≡N chains. The C–N distances range from 1.13(1) to 1.17(1) Å. All cyanide groups coordinate in the usual linear fashion with deviations from linearity less than 8°.

The metal–metal separations of 2.691(1) and 2.794(1) Å with the acute MoSMo angles ranging from 67.07(6)° to 72.91(7)°, together with the observed diamagnetism, are taken as indications of metal–metal bonding [32]. For the phosphonium salt, this Mo–Mo distance is 2.730(4). A comparison of these Mo–Mo distances with those found in the other structures (2.50–2.90 Å for the single bond distances), combined with the observed diamagnetism and the number of metal electrons available, shows that the Mo–Mo bonding scheme is best regarded as

TABLE III. Selected Bond Lengths and Angles in the $[Mo_2(\mu_4\text{-}S_2)(\mu_2\text{-}SO_2)(CN)_8]^{4-}$ Ion[a].

A. Bond lengths (Å)							
Mo1–C11	2.168(10)	Mo2–C21	2.128(9)	Mo3–C31	2.151(9)	Mo4–C41	2.147(10)
Mo1–C12	2.147(9)	Mo2–C22	2.178(9)	Mo3–C32	2.160(9)	Mo4–C42	2.157(9)
Mo1–C13	2.153(9)	Mo2–C23	2.116(10)	Mo3–C33	2.164(10)	Mo4–C43	2.166(9)
Mo1–C14	2.148(9)	Mo2–C24	2.163(9)	Mo3–C34	2.153(9)	Mo4–C44	2.135(10)
Mo1–S11	2.366(2)	Mo2–S11	2.371(2)	Mo3–S31	2.351(2)	Mo4–S31	2.351(2)
Mo1–S12	2.442(2)	Mo2–S12	2.429(2)	Mo3–S32	2.450(2)	Mo4–S32	2.440(2)
Mo1–S13	2.432(2)	Mo2–S13	2.432(2)	Mo3–S33	2.443(2)	Mo4–S33	2.441(2)
S11–O11	1.486(6)	S12–S13	2.000(3)	S31–O31	1.489(7)	S32–S33	1.999(3)
S11–O12	1.489(6)			S31–O32	1.504(7)		
C11–N11	1.13(1)	C21–N21	1.17(1)	C31–N31	1.14(1)	C41–N41	1.17(1)
C12–N12	1.14(1)	C22–N22	1.13(1)	C32–N32	1.14(1)	C42–N42	1.13(1)
C13–N13	1.14(1)	C23–N23	1.17(1)	C33–N33	1.14(1)	C43–N43	1.14(1)
C14–N14	1.14(1)	C24–N24	1.13(1)	C34–N34	1.14(1)	C44–N44	1.14(1)
Mo1···Mo2	2.691(1)			Mo3···Mo4	2.794(1)		

(continued on facing page)

TABLE III *(continued)*

B. Bond angles (deg)

Mo1–C11–N11	175.1(9)	Mo2–C21–N21	177.2(8)	Mo3–C31–N31	175.0(8)	Mo4–C41–N41	179.0(9)
Mo1–C12–N12	177.0(8)	Mo2–C22–N22	174.9(9)	Mo3–C32–N32	175.4(9)	Mo4–C42–N42	177.1(8)
Mo1–C13–N13	177.4(8)	Mo2–C23–N23	176.0(1.1)	Mo3–C33–N33	175.6(9)	Mo4–C43–N43	173.2(9)
Mo1–C14–N14	176.0(9)	Mo2–C24–N24	175.6(9)	Mo3–C34–N34	172.8(9)	Mo4–C44–N44	177.0(10)
S11–Mo1–S12	105.88(8)	S11–Mo2–S12	106.17(8)	S31–Mo3–S32	102.39(7)	S31–Mo4–S32	102.66(7)
S11–Mo1–S13	106.83(8)	S11–Mo2–S13	106.69(8)	S31–Mo3–S33	104.24(8)	S31–Mo4–S33	104.29(8)
S12–Mo1–S13	48.44(7)	S12–Mo2–S13	48.59(7)	S32–Mo3–S33	48.24(8)	S32–Mo4–S33	48.36(8)
S11–Mo1–C11	164.5(2)	S11–Mo2–C21	87.3(3)	S31–Mo3–C31	90.0(2)	S31–Mo4–C41	90.3(3)
S11–Mo1–C12	88.5(2)	S11–Mo2–C22	164.3(3)	S31–Mo3–C32	82.2(3)	S31–Mo4–C42	88.5(2)
S11–Mo1–C13	80.3(2)	S11–Mo2–C23	81.4(3)	S31–Mo3–C33	88.6(2)	S31–Mo4–C43	162.7(3)
S11–Mo1–C14	92.1(3)	S11–Mo2–C24	87.7(3)	S31–Mo3–C34	165.1(2)	S31–Mo4–C44	79.1(3)
S12–Mo1–C11	88.0(2)	S12–Mo2–C21	129.2(3)	S32–Mo3–C31	128.6(2)	S32–Mo4–C41	127.8(3)
S12–Mo1–C12	81.3(2)	S12–Mo2–C22	88.8(3)	S32–Mo3–C32	156.1(3)	S32–Mo4–C42	79.5(2)
S12–Mo1–C13	155.5(2)	S12–Mo2–C23	154.1(3)	S32–Mo4–C33	81.4(3)	S32–Mo4–C43	93.1(3)
S12–Mo1–C14	127.7(2)	S12–Mo2–C24	80.8(3)	S32–Mo3–C34	90.3(3)	S32–Mo4–C44	156.4(3)
S13–Mo1–C11	87.5(2)	S13–Mo2–C21	80.6(3)	S33–Mo3–C31	80.4(2)	S33–Mo4–C41	79.5(3)
S13–Mo1–C12	129.6(2)	S13–Mo2–C22	86.6(2)	S33–Mo3–C32	153.8(3)	S33–Mo4–C42	127.7(2)
S13–Mo1–C13	153.4(2)	S13–Mo2–C23	153.9(3)	S33–Mo3–C33	129.5(2)	S33–Mo4–C43	91.4(3)
S13–Mo1–C14	79.5(2)	S13–Mo2–C24	129.3(3)	S33–Mo3–C34	89.9(3)	S33–Mo4–C44	154.6(3)
C11–Mo1–C12	86.8(3)	C21–Mo2–C23	74.9(4)	C31–Mo3–C34	87.8(3)	C41–Mo4–C44	75.3(4)
C12–Mo1–C13	75.2(3)	C23–Mo2–C24	74.8(4)	C31–Mo3–C32	74.2(3)	C42–Mo4–C44	77.1(4)
C13–Mo1–C11	84.1(3)	C22–Mo2–C23	83.0(4)	C32–Mo3–C34	83.0(4)	C43–Mo4–C44	83.6(4)
C11–Mo1–C14	84.4(3)	C21–Mo2–C22	86.7(3)	C33–Mo3–C34	85.8(3)	C41–Mo4–C43	85.4(4)
C13–Mo1–C14	74.5(3)	C22–Mo2–C24	90.2(3)	C32–Mo3–C33	75.2(4)	C42–Mo4–C43	87.5(3)
O11–S11–O12	109.3(4)	Mo1–S11–Mo2	69.25(6)	O31–S31–O32	106.9(4)	Mo3–S32–Mo4	69.70(6)
Mo1–S12–Mo2	67.07(6)	Mo1–S13–Mo2	71.19(6)	Mo3–S31–Mo4	72.91(7)	Mo3–S33–Mo4	69.80(7)

[a]Estimated standard deviations are given in parentheses.

consisting of a single bond. There is uncertainty in assigning metal–metal bond orders since extensive mixing by metal–ligand and metal–metal bonding interactions can exist.

Electronic and Vibrational Spectra

The absorption spectrum (Fig. 2) of complex (*2*) shows a rather strong band in the visible region centered at 550 nm ($\epsilon \simeq 4000$ mol^{-1} l^{+1} cm^{-1}) and weaker bands at 410 (sh) and 340 nm ($\epsilon \simeq 2500$ mol^{-1} l^{+1} cm^{-1}). A variable temperature experiment has shown that the intensity of the 550 nm band remains constant in the 300–80 K range, thus establishing the allowed character of the corresponding transition. It is involved in a resonance Raman effect (*vide infra*) so that its assignment may help to assign the Raman spectrum (and *vice versa*).

The Mo–CN charge transfer transitions (C.T.) are expected at *ca.* 30 000 cm^{-1}, as calculated from the optical electronegativities of Mo^{III} and CN^- [33]. This is in agreement with the data for $K_4[Mo(CN)_7]\cdot 2H_2O$ where the Mo → CN C.T. transitions are located at 31 000 cm^{-1} and higher [34]. According to Müller *et al.* [35], C.T. transitions of the type S_2^{2-} → metal should be located at *ca.* 20 000 cm^{-1}; in the case of disulfur bridged complexes this transition might be at higher energy, the low energy transition then being assigned to the metal–metal moiety. Little is known of metal–SO_2 charge transfer transitions. From the above data it follows that the 18 200 cm^{-1} (550 nm) transition most likely involves the 'Mo_2S_2' moiety: it may be assigned either to the S_{Π^*} → Mo C.T. transition or to the Mo–Mo σ–σ^* transition.

Intraligand vibrations can be easily located on the IR spectrum at 2120, 2127 and 2135 cm^{-1} for the CN stretching modes; 1167 and 1040 for the SO stretching modes and 520 cm^{-1} for the S–S stretching mode. Among these, only the CN stretching vibrations (2140 cm^{-1}, weak) are seen on the Raman spectrum which is dominated by a set of 6 rather strong bands in the 500–200 cm^{-1} region (Fig. 3). All these bands are polarized ($\rho = 0.33$). They all exhibit resonance enhancement when excited within the 18 200 cm^{-1} electronic transition. The excitation profiles of these vibrations have been measured and are plotted in Fig. 4. They make it possible to discriminate between the different vibrations: the 461 and 318 cm^{-1} modes are weakly enhanced in much the same way as the CN stretching mode, whereas the four remaining modes at 195, 347, 383 and 428 cm^{-1} are more strongly enhanced. For this reason,

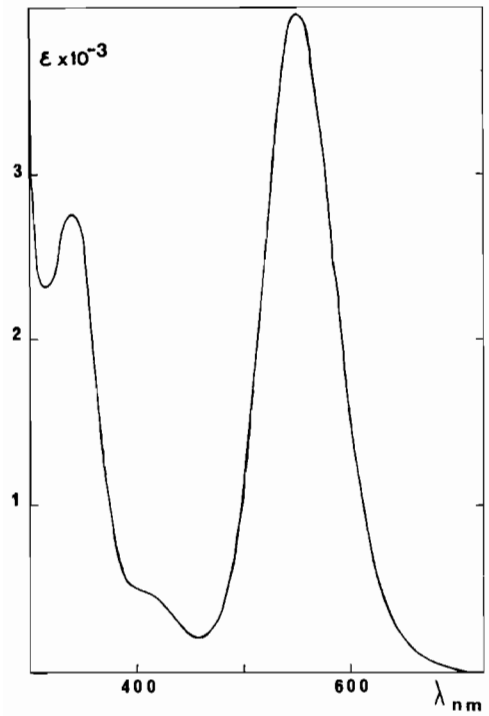

Fig. 2. Absorption spectrum of (*2*) in $H_2O/CH_3OH(3:1)$ solution.

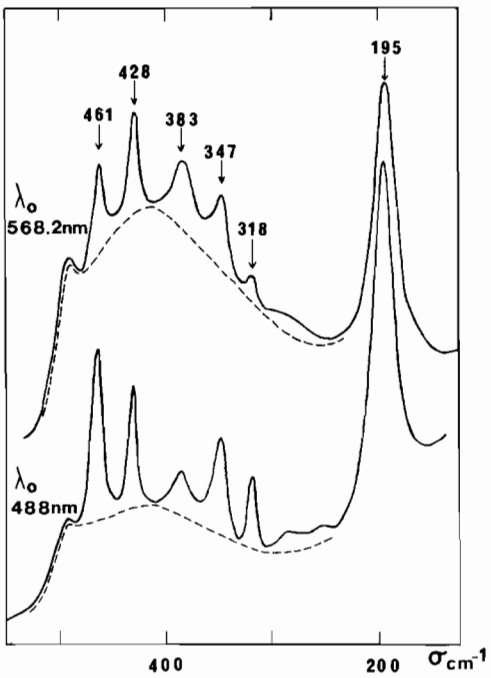

Fig. 3. Raman spectrum of (*2*) in $H_2O/CH_3OH(3:1)$ solution. Lower trace: $\lambda_o = 488$ nm, upper trace $\lambda_o = 568.2$ nm; intensities × 1/4. Dashed line: background due to the quartz cell.

we consider the latter as vibrational modes of the Mo_2S_2 chromophore. The strong intensity and low frequency of the 195 cm^{-1} mode are in favor of its

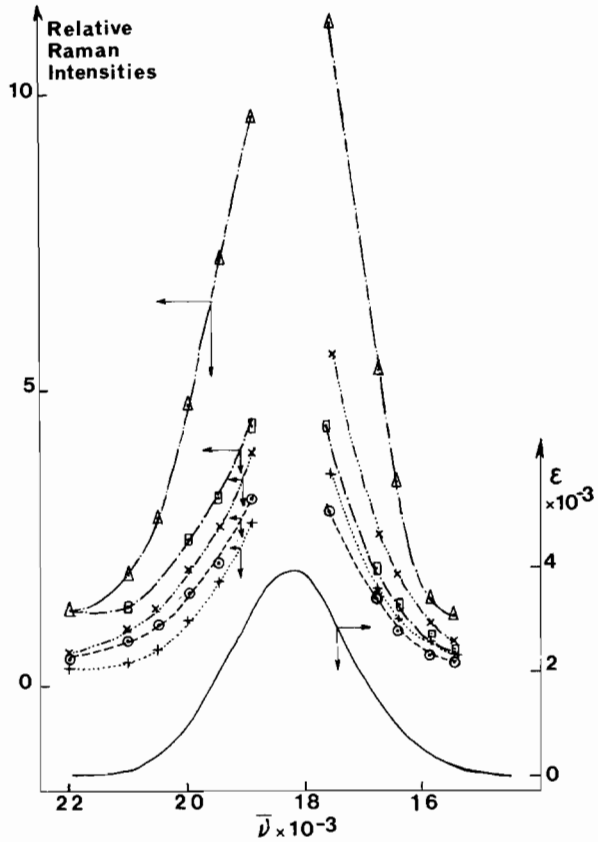

Fig. 4. Relative Raman intensities of the low frequency modes of (*2*) *versus* exciting frequencies: + 383 cm^{-1} mode; ⊙ 347 cm^{-1} mode; × 428 cm^{-1} mode; ▣ 461 cm^{-1} mode; △ 195 cm^{-1} mode. At the lowest is the absorption spectrum of (*2*).

assignment to the Mo–Mo stretching vibration (it should be noted that the metal stretching vibration is probably coupled with Mo–S vibrations). This is comparable to the band observed at 197 cm^{-1} for $[Mo_3S_{13}]^{2-}$ which was assigned [36] to the Mo–Mo stretching on the basis of isotopic substitution (the Mo–Mo distances are almost identical in the two complexes).

The other low frequency Raman modes are located in the region of metal-sulfur and metal cyanide vibrations. Taking into account the excitation profiles, we assign tentatively the 461 and 318 cm^{-1} bands to Mo–CN vibrations and the 347, 383 and 428 cm^{-1} bands to Mo–S vibrations.

Trial calculations of the excitation profiles have been performed based either on a single resonant electronic state (A term scattering) [37] or on the coupling of two resonant electronic states (B term scattering) [37]. The excitation profiles of the 195, 347, 383 and 428 cm^{-1} bands are best represented by A-term scattering involving the 18 200 cm^{-1} transition, whereas the excitation profiles of the 461 and 318 cm^{-1} bands are best represented by B-term

scattering, involving the 18 200 cm^{-1} and a higher energy transition at *ca.* 30 000 cm^{-1}. But in neither case were we able to get a good fit close to the absorption maximum.

This study gives a clear evidence of the metal-to-metal bond in the anion $[Mo_2(\mu_4\text{-}S_2)(\mu_2\text{-}SO_2)(CN)_8]^{4-}$ in which the metal atoms are also bridged by ligands.

Acknowledgement

We thank Dr. J. Lomas for correcting the manuscript.

References

1 J. E. Lyons, 'Aspects of Homogeneous Catalysis', R. Ugo, Ed., *3*, D. Reidel Publishing Company, 3 (1977).
2 R. D. Jones, D. A. Summerville and F. Basolo, *Chem. Rev., 79*, 139 (1979).
3 L. Vaska, *Accounts Chem. Res., 9*, 175 (1976).
4 J. S. Valentine, *Chem. Rev., 73*, 235 (1973).
5 G. R. John, B. F. Q. Johnson, J. Lewis and K. C. Wong, *J. Organometal. Chem., 169*, C23 (1979).
6 R. Ugo, S. Bhaduri, B. F. G. Johnson, A. Khair, A. Pickard and Y. Ben Taarit, *J. Chem. Soc. Chem. Commun.*, 695 (1976).
7 S. D. Pell and J. N. Armor, *J. Am. Chem. Soc., 97*, 5012 (1975).
8 S. Cenini, F. Porta and M. Pizzotti, *J. Mol. Cat., 15*, 297 (1982).
9 M. H. Chisholm, K. Folting, J. C. Huffman and Ch. C. Kirkpatrick, *J. Chem. Soc. Chem. Commun.*, 189 (1982).
10 L. Markó, B. Markó-Monostory, Th. Madach and H. Vahrenkamp, *Angew. Chem. Int. Ed. Engl., 19*, 226 (1980).
11 C. Potvin, J.-M. Brégeault and J.-M. Manoli, *J. Chem. Soc. Chem. Commun.*, 664 (1980).
12 M. G. B. Drew, *Progress in Inorg. Chem., 23*, 67 (1977).
13 C. D. Garner, *Coord. Chem. Rev., 45*, 153 (1982).
14 W. C. Trogler and H. B. Gray, *Accounts Chem. Res., 11*, 232 (1978).
15 F. A. Cotton, *J. Mol. Struct., 59*, 97 (1980).
16 F. A. Cotton, *J. Less-Common Metals, 54*, 3 (1977).
17 R. N. McGinnis, T. R. Ryan and R. E. McCarley, *J. Am. Chem. Soc., 100*, 7900 (1978).
18 M. H. Chisholm and F. A. Cotton, *Accounts Chem. Res., 11*, 356 (1978).
19 R. D. Wilson, S. A. Graham and R. Bau, *J. Organometal. Chem., 91*, C49 (1975).
20 R. G. Teller, R. G. Finke, J. P. Collman, H. B. Chin and R. Bau, *J. Am. Chem. Soc., 99*, 1104 (1977).
21 K. N. Raymond, P. W. R. Corfield and J. A. Ibers, *Inorg. Chem., 7*, 1362 (1968).
F. A. Jurnak and K. N. Raymond, *Inorg. Chem., 13*, 2387 (1974).
22 M. G. B. Drew, P. C. H. Mitchell and C. F. Pygall, *Angew. Chem., Int. Ed. Engl., 15*, 784 (1976); *J. Chem. Soc., Dalton Trans.*, 1213 (1979).
23 R. H. Blessing, P. Coppens and P. Becker, *J. Appl. Cryst., 7*, 488 (1972). A local modified version of this program is employed using the Lehman-Larsen algorithm. M. S. Lehman and F. K. Larsen, *Acta Crystallogr., Sect. A, A 30*, 580 (1974).
24 P. Main, L. Lessinger, M. M. Woolfson, G. Germain and J. P. Declercq, 'MULTAN. A system of Computer Programs for the Automatic Solution of Crystal Structures from X-ray Diffraction Data'. Universities of York (G.B.) and Louvain (Belgium) 1977.
25 All calculations have been performed by using the CH IRIS 80 computer of the Atelier d'Informatique. In addition to various local programs, modified versions of the following were employed: Zalkin's FORDAP Fourier summation program; Johnson's ORTEP thermal ellipsoid plotting program; Busing and Levy's ORFFE error function program; Ibers' NUCLS full-matrix program which in its nongroup form closely resembles the Busing and Levy's ORFLS program.
26 The function minimized was $\Sigma w(|F_o| - |F_c|)^2$ where $w = 4F_o^2/\sigma^2(F_o^2)$. The unweighted and weighted residuals are defined as follows: $R = (\Sigma||F_o| - |F_c||)/\Sigma|F_o|$ and $R_w = [\Sigma w(|F_o| - |F_c|)^2/\Sigma w|F_o|^2]^{1/2}$.
27 D. T. Cromer and J. T. Waber, 'International Tables for X-Ray Crystallography'; Kynoch Press: Birmingham, England, 1974, Vol. IV, Table 2.2A and 2.3.1.
28 R. R. Ryan, G. J. Kubas, D. C. Moody and P. G. Eller, *Structure and Bonding, V46*, 47 (1981).
29 M. R. Churchill and K. L. Kalra, *Inorg. Chem., 12*, 1650 (1973).
30 A. Müller and W. Jaegermann, *Inorg. Chem., 18*, 2631 (1979).
31 A. Müller, W. O. Nolte and B. Krebs, *Inorg. Chem., 19*, 2835 (1980).
32 D. J. Miller, R. C. Haltiwanger and M. Rakowski-Dubois, 'Proceedings of the Climax Fourth International Conference on the Chemistry and Uses of Molybdenum', H. F. Barry and P. C. H. Mitchell eds, Climax Molybdenum Company, Ann Arbor, Michigan, 1982, p. 348.
33 A. B. P. Lever, 'Inorganic Electronic Spectroscopy', Elsevier, Amsterdam, ch. 8, 244 (1968).
34 H. B. Gray, *Inorg. Chem., 12*, 825 (1973).
35 A. Müller, W. Jaegermann and G. H. Enemark, *Coord. Chem. Rev., 46*, 245 (1982).
36 A. Müller, R. Jostes, W. Jaegermann and R. G. Bhattacharyya, *Inorg. Chim. Acta, 41*, 259 (1980).
37 T. G. Spiro and P. Stein, *Ann. Rev. Phys. Chem., 28*, 501 (1977).